

# Cyclic Demand at the Shell-Bottom Connection of Unanchored Steel Tanks



**G. Cortes**

*LeTourneau University, Longview, Texas*

**G.S. Prinz & A. Nussbaumer**

*Ecole Polytechnique Fédérale de Lausanne, Switzerland*

**M.G. Koller**

*Résonance Ingénieurs-Conseils SA, Switzerland*

## SUMMARY:

Unanchored steel tanks may rock under strong ground motion, causing cycles of uplift at the shell-base welded connection. These cycles of uplift may lead to fracture of this connection, resulting in spillage of the content. The rotational capacity of the shell-base connection can be determined from curves of rotation vs. number of cycles to failure, determined experimentally (Cortes and Nussbaumer, 2011; Prinz and Nussbaumer, 2012). In order to use these curves, the maximum number of cycles at the shell-base connection needs to be estimated for the earthquake hazard of the site of interest. This paper presents a model for estimating the number of expected cycles of rotation at the shell-base connection. The model was then used for the earthquake hazard of Sion, Switzerland, resulting in 4 equivalent amplitude cycles. The RN curve shows that for 4 cycles of rotation, typical shell-base connections may sustain rotations greater than 0.4 radians.

*Keywords: Unanchored steel tanks, shell-base connection, rotation limit, seismic demand, low-cycle fatigue*

## 1. INTRODUCTION

Gasoline and other oil byproducts are commonly stored in steel tanks that rest on ground without any anchorage. Under strong motion, the impulsive mass of the contained liquid generates a moment about the base of the tank capable of causing partial uplift of the base (see Figure 1). Uplifting of the base is accompanied by a distortion of the shell-base welded connection, capable of inducing low-cycle fatigue failure. Failure of this connection would have serious repercussions when the liquid contained is hazardous to the environment. Current codes of standard practice such as the Eurocode (Eurocode-8, 1998) and New Zealand's Recommendations (NZSEE, 2009) address this issue by limiting the amount of rotation at the connection to 0.2 radians. Recent research by Cortes et al. (2011) and Prinz and Nussbaumer (2012) suggest that this limit is overly conservative and that a limit of 0.4 radians is better justified. Cortes et al. and Prinz and Nussbaumer tested shell-base connections with different thicknesses and of different steel grades, new and from existing tanks, under cyclic loading. From these experiments curves of rotation vs. number of cycles to failure (RN curves), similar to fatigue life curves, were created. Figure 2 shows one of the specimens being tested (left) and one of the RN curves created (right). The RN curve shown was created from experiments of new specimens, with base plate thicknesses of 6, 8 or 10mm, made from S355 steel. Data points from the experiments are indicated in the RN curve by the blank dots. This plot also shows median (50% confidence) and 95% confidence curves.

The RN curves provide the number of cycles required to fail the connection for different levels of rotation. This curve can be regarded as the capacity curve of the shell-base connection. In order to use this curve, it is necessary to estimate the number of cycles at the connection. An estimate of the number of cycles was made by means of finite element analysis (FEA) for a limited number of ground motion records (Cortes and Nussbaumer, 2010). While FEA is ideal for this type of highly nonlinear analysis involving material and geometrical nonlinearities, and soil-structure interaction, the computational time to run each ground motion and the amount of data generated was very large,

limiting the amount of ground motions used for the time history analysis. For this reason, a simplified model, capable of capturing the dynamic effects of a rocking tank was sought. Different mathematical models have been proposed for the analysis of unanchored tanks. One such model was developed by Malhotra and presented in a series of three papers (Malhotra and Veletsos, 1994a; Malhotra and Veletsos, 1994b; Malhotra and Veletsos, 1994c). While such model agreed well with FEA, its convergence was greatly dependent on the time step used and therefore was difficult to implement. For this reason, the authors developed an alternative model and implemented it in the analysis software OpenSees (Mazzoni et al., 2006).

This paper presents the simplified model of the tank in Section 2. Section 3 discusses the time history analysis used to estimate the number of cycles of rotation. Results of the analysis and conclusions are presented in Section 4 and 5, respectively.

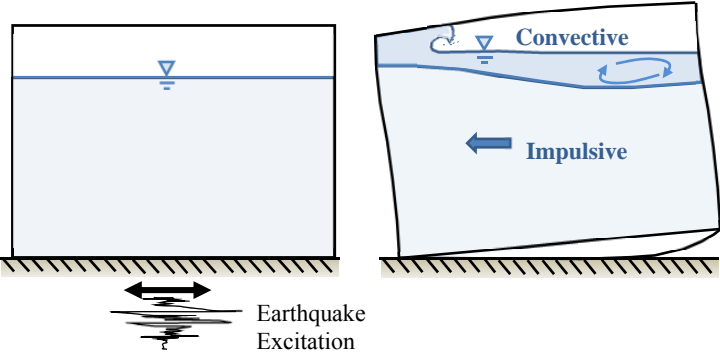


**Figure 1.** Tank at rest (left); uplifted tank showing the impulsive and convective liquid masses (right).

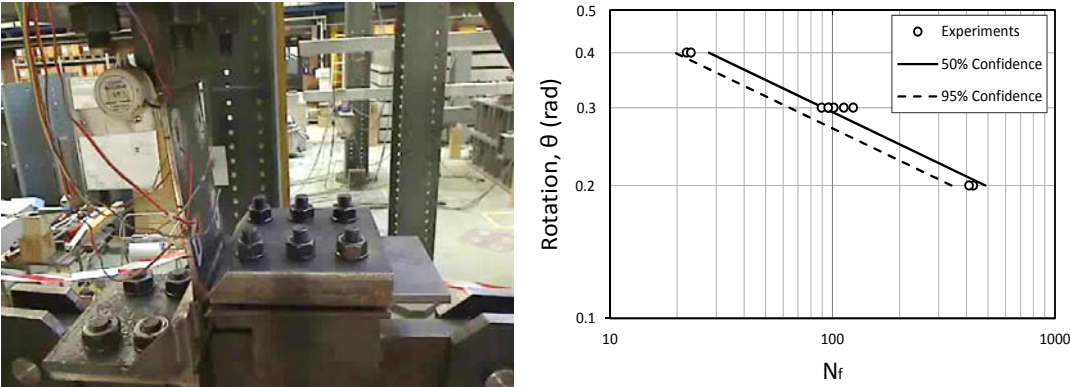


**Figure 2.** Shell-base connection test (left); rotation vs. number of cycles to failure curve (RN curve) (right).

**2. SIMPLIFIED MODEL**

The simplified model consists of a multiple-degree of freedom (MDF) system capable of predicting the behavior of the tank whether the tank base is in full contact with the ground or partially uplifted. This model was calibrated to match the moment-rotation curve given by the NZSEE (2009). The model used is illustrated in Figure 3.

Only the impulsive mass was considered since this portion of the total liquid mass is mainly responsible for causing rocking of the tank under strong shaking. The mass is located at a height,  $h_i$ , determined according to the NZSEE (2009). The base of the tank is modeled by means of two rigid links, each having a length equal to the tank radius. A rigid base was used since it has been shown that the base of the tank wall rotates as a rigid body due to the high in-plane stiffness of the shell (Fujikazu et al., 1988). The weight of the tank is assigned as a concentric load at the center of the tank base,

where the ‘column’ joins the base. Three zero-length vertical springs and one horizontal spring are located at both ends of the tank (nodes 3 and 5 in Figure 3). The vertical springs account for the stiffness of the soil and the uplift resistance provided by the weight of the liquid being uplifted. The combined behavior of the vertical springs working in parallel is shown in Figure 3 (right). Note that the uplift resistance (quadrant I in Figure 3 right), is provided by the weight of the liquid been displaced upward and is represented by a bilinear curve. The compressive capacity, representing the stiffness of the ground, has a very high stiffness, indicating that no soil penetration is allowed. This was the condition of most tanks found in Switzerland as they commonly rest on a concrete slab. The compressive stiffness could be adjusted to accommodate different soil conditions and to allow ground penetration. The horizontal springs are compression only springs used to transfer the horizontal acceleration applied at the base of the tank (nodes 1 and 2). Since only one end (node 1 or 2) is under compression at any given time, the other end is experiencing tension and is capable of undergoing uplift.

Under small base accelerations, the overturning moment generated by the impulsive mass is not large enough to cause rocking of the base. Thus, the tank does not undergo rocking and works as a single-degree-of-freedom (SDF) system with a fixed end at node 4. Before uplift takes place only the weight of the tank contributes to resisting the overturning moment. This resistance is given by Equation 2.1.

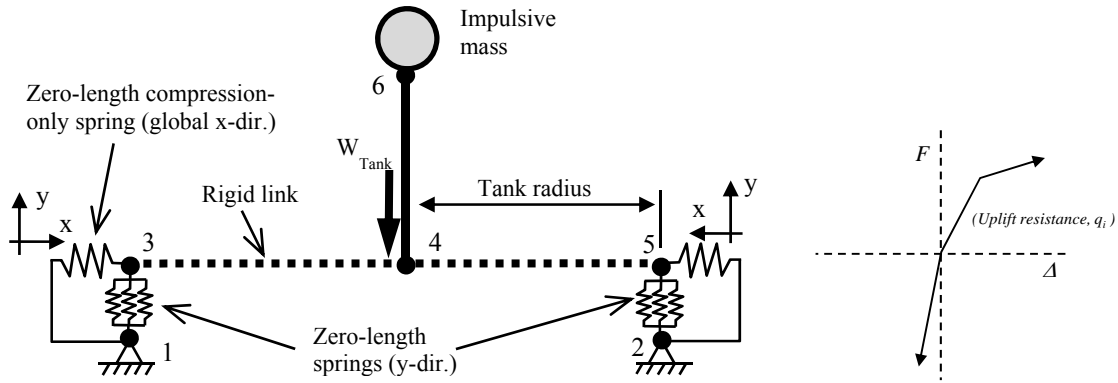


**Figure 3.** Simplified model used for non-linear time history analysis (left); non-linear force-uplift curve used for springs (right).

Once the base acceleration is strong enough to cause an overturning moment greater than the resisting moment (given by Equation 2.1), rocking occurs. That is represented by point 1 in Figure 4, which shows the moment-rotation curve obtained by following NZSEE (2009) for an unanchored tank located in Rümlang, Switzerland (see Table 2.1). Figure 4 also shows the moment-rotation ( $\psi$ ) curve used in the model. Note that points two and three are calibrated to match the NZSEE curve at connection rotations of  $\theta = 0.1$  and  $0.14$  radians, corresponding to a base rotation ( $\psi$ ) of  $0.005$  and  $0.0325$  radians.

Once the moment-deformation curve is developed, the force vs. uplift relationship used for the springs is determined by establishing equilibrium of forces, as shown in Figure 5. The resulting resistance force,  $q_i$ , is determined from Equation 2.2. This force accounts for the weight of the liquid above the portion of the base plate that is being uplifted from the ground and therefore, acts as a restoring force bringing the tank back into full contact with the ground.

$$M_{res1} = (W_{wall} + W_{roof})R \quad (2.1)$$

$$q_i = \frac{Porhi - (W_{wall} + W_{roof})R}{2R} \quad (2.2)$$

In Equation 2.2, the overturning force,  $P_{OT}h_i$ , is taken as the  $M_{OT}$  from NZSEE (2009), as shown in Figure 4 (points 2 and 3). The uplift distance may be obtained from the geometry of the uplifted tank, as given by Equation 2.3. Figure 4 (right) shows the resulting force vs. uplift curve used for the tension springs, for the Rüm-lang tank.

$$\delta_i = 2R\psi \quad (2.3)$$

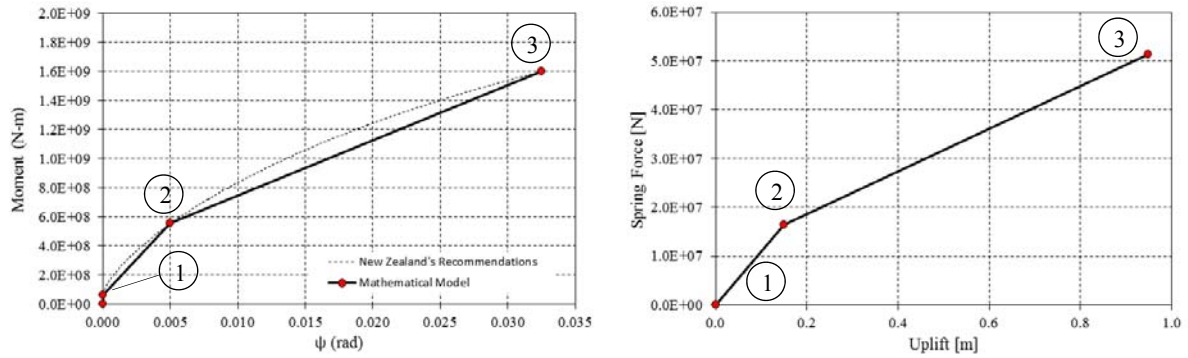


**Figure 4.** Moment vs. base rotation curve (left); force vs. uplift displacement curve for the spring (right).

**Table 2.1.** Main parameters for the tanks studied.

Tank	H	R	H/R	Volume (m <sup>3</sup> )	Mass (kg)	$h_i$ (m)
Rüm-lang	26.3	15	1.75	18,600	10988705	13.0
Mellingen	25	22	1.14	38,000	18349542	10.5

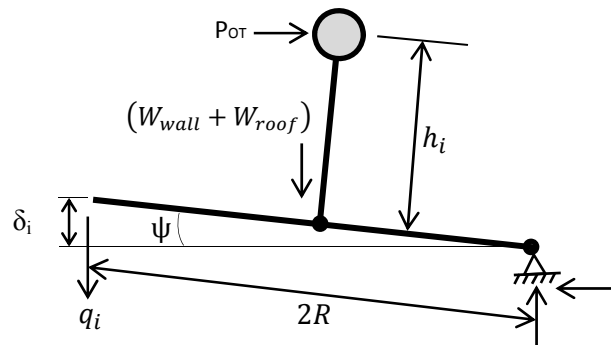


**Figure 5.** Simplified model undergoing rocking.

Results from the simplified model were compared with results from a robust finite element analysis (FEA) performed by Cortes and Nussbaumer (2010). The displacement history of the simplified model, analyzed in OpenSees (Mazzoni et al., 2006), and for the finite element model, analyzed in ABAQUS, are shown in Figure 6. For more details of the FEA see Cortes and Nussbaumer (2010). It can be seen that the simplified model correlates well with the robust FEA.

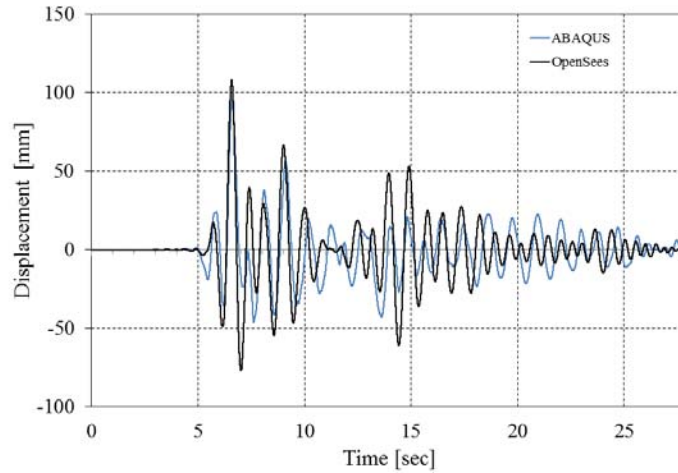


**Figure 6.** Tank displacement history from ABAQUS and from the simplified model.

### 3. ANALYSIS

The model shown in Section 2 was used to perform a time history analysis of two tanks located in Switzerland. The main properties of each tank are given in Table 2.1. Because of the lack of recorded strong motion in Switzerland, artificial ground motions generated using the procedure by Sabetta and Pugliese (1996) were used. This procedure generates ground motions empirically based on ground motion prediction equations from earthquakes recorded in Italy. The ground motions were generated to match, on average, the design spectrum for Sion, Switzerland, which has the highest earthquake hazard in Switzerland. Figure 7 shows the median response spectrum from the 50 generated ground motions along with the design spectrum for Sion, with a soil class C (Eurocode-8, 1998). Note the good correlation between the design and median spectrum, indicating that the applied ground motions represent expected site accelerations. Parameters considered for the synthetic ground motion generation include: deep soils, earthquake magnitude of M7.2, and an epicentral distance of 22km. This figure also shows 5 of the 50 earthquakes generated. 10% Rayleigh damping was used in the first and second mode for the simplified model.

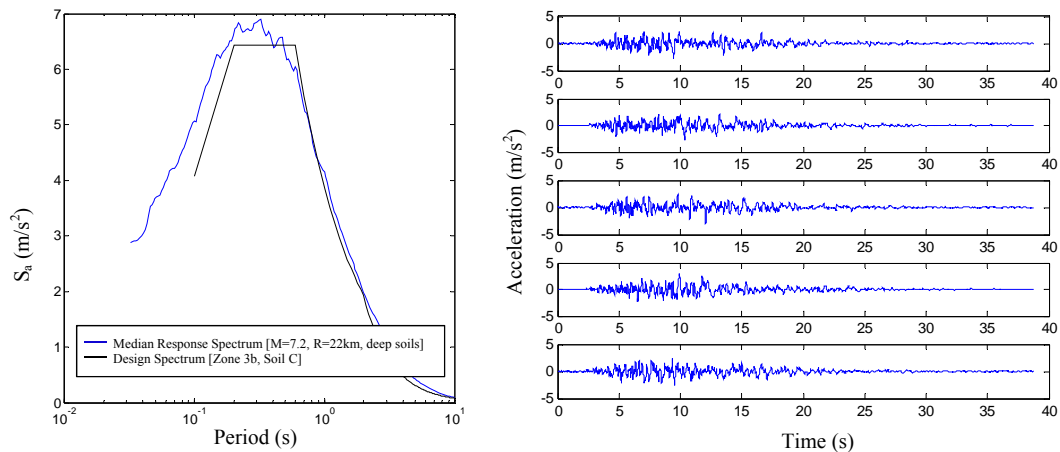


**Figure 7.** Median response spectrum for the 50 generated ground motions plotted along with the design spectrum for a seismic zone 3b and a soil C (left); 5 of the 50 generated ground motions (right).

From the analysis performed, the uplift histories of the left and right ends of the tank were obtained. The shell-base rotation was calculated by means of Equation 3.1 (Eurocode-8, 1998).

$$\theta = \frac{2v}{L} - \frac{v}{2R} \quad (3.1)$$

where  $v$  is the uplifted height,  $L$  is the uplifted length, and  $R$  is the radius of the tank. The uplifted length is determined according to the method used by NZSEE (2009).

When determining the cyclic demand in the connection, it is necessary to use principles that allow for the transformation from a rotation history of cycles with different amplitude into a history of cycles with uniform amplitude. This was accomplished by assuming that each cycle causes a certain amount of damage which is linearly proportional to the rotation in the connection (Miner, 1945) and that there is a power relationship between the number of cycles applied and the amplitude of the rotation applied (Coffin, 1954; Manson, 1954). Combining these two assumptions, Equation 3.2 was derived.

$$N_{f\theta} = \sum_{i=1}^n \left( \frac{\theta_i}{\theta} \right)^c \quad (3.2)$$

In Equation 3.2,  $N_{f\theta}$  is the equivalent number of cycles at a constant rotation angle,  $\theta$ ;  $\theta$  is the rotation at which it is desired to calculate the number of equivalent cycles;  $\theta_i$  is the rotation magnitude at each cycle of the response history and  $c$  is slope of the RN curve (obtained experimentally, see Figure 2). The rotation response history of each ground motion was converted into equivalent histories of cycles with amplitude equal to the maximum rotation recorded in that particular ground motion (Malhotra, 2002).

The assumption of linear damage (Miner's rule) is widely known to have some limitations (Krawinkler et al., 1983). Nevertheless, it was adopted in this investigation for its simplicity.

#### 4. RESULTS

The time history analysis was performed for two tanks, for the 50 ground motions, resulting in 100 uplift histories, for each end (left and right) of the tank. Figure 8 shows one of the 50 generated ground accelerations along with the displacement response and the uplift history for the left and right ends of the tank. Note that the displacement response shows the fixed (anchored) tank condition and the unanchored tank condition. Initially these two undergo similar deformations, but as soon as the overturning moment is greater than the resisting moment the tank undergoes rocking, causing significantly greater displacements for the rocking tank as compared to the anchored tank. Figure 8 (right) shows a probability density function (PDF) for the combined results of the time history analysis of the two tanks, for the left and right ends of the tanks, for a total of 200 cases. This figure also shows the median value for the number of cycles which corresponds to 2 cycles and the 95<sup>th</sup> percentile which corresponds to nearly 4 cycles.

By combining the estimated number of cycles of rotation at the connection with the capacity curves obtained experimentally (see Figure 2), it can be seen that the estimated 4 cycles would yield a rotation higher than the maximum tested of 0.4 radians. This investigation suggests that a limit of 0.4 radians is more realistic than the existing 0.2 radians given by the Eurocode-8 (1998) and by the NZSEE (2009). It should be noted that the capacity curves were developed for tanks representing the common practice in Switzerland and that the estimated number of cycles was estimated for the earthquake hazard of Sion, Switzerland.

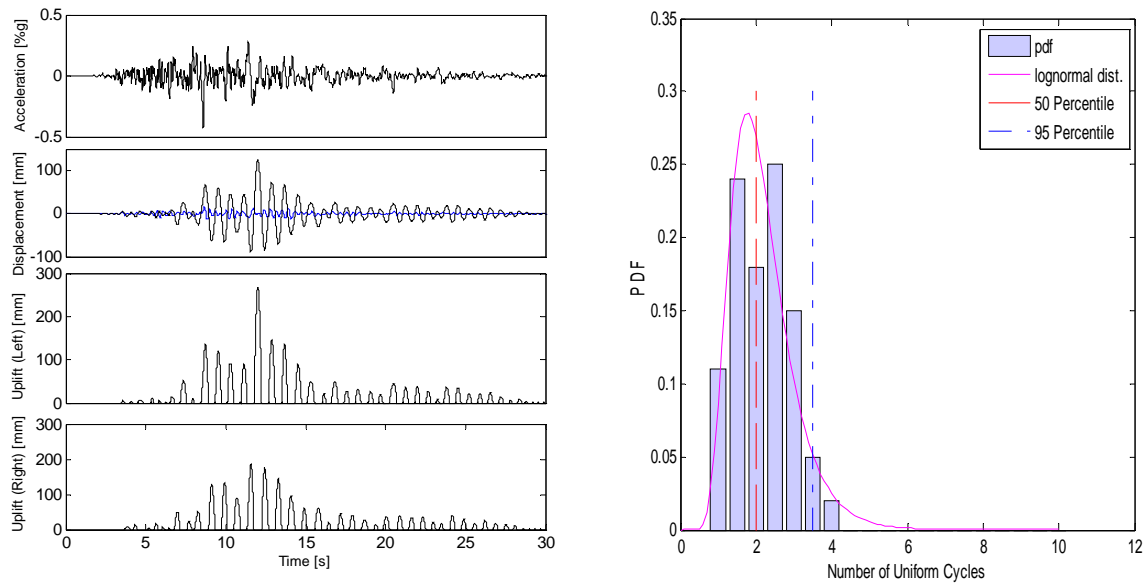


**Figure 8.** Time history results for 1 of the 50 ground motions, for the Rümlang tank (left); PDF for the 200 cases (right).

## 5. SUMMARY AND CONCLUSIONS

Under strong ground motion, unanchored tanks may rock and undergo cycles of uplift at the base plate. Uplift of the base plate is accompanied by distortion of the shell-base welded connection, which may lead to fracture of this connection. Current codes (Eurocode-8, 1998; NZSEE, 2009) address this limit state by limiting the amount of rotation of this connection to 0.2 radians. This limit was based on a series of assumptions rather than on experimental work. For that reason, an extensive experimental work was conducted and capacity curves were created (RN curves) (Cortes and Nussbaumer, 2011; Prinz and Nussbaumer, 2012). Once capacity curves were generated, it was necessary to determine the number of cycles of rotation expected at the shell-base connection, for the seismic hazard of Switzerland. This paper presented a simplified model used for estimating this number of equivalent cycles of rotation.

The simplified model described in this paper consisted of a column (tank walls) attached to rigid links (tank base) at the base. The base was attached to the ground with a series of springs which accounted for the stiffness of the soil and the liquid being uplifted when the tank is undergoing rocking motion. The model was used for the time history analysis performed in OpenSees (Mazzoni et al., 2006). While the simplified model estimates base uplift height, determining uplift length for the connection rotation calculation still required code methods. Comparison of the simplified model with a robust FEA performed in ABAQUS (Cortes and Nussbaumer, 2010) showed good correlation. From the time history analysis, the expected number of equivalent magnitude cycles was found to be about 4 cycles. Entering the rotation vs. number of cycles curve (RN curve) with 4 cycles indicates that the rotational capacity of the connection is greater than 0.4 radians. This is twice the rotation limit given by the Eurocode-8 and NZSEE, indicating that these two methods are over conservative. The number of cycles in this study was estimated for the seismicity of Sion, Switzerland. It should be noted that the RN curve is based on experimental work, using specimens from tanks found in Switzerland. Recent experimental findings suggest large shifts in the RN curves depending on base-plate ductility (Prinz and Nussbaumer, 2012). Additionally, due to tank fabrication methods, there are sections of base-plate having transverse welds at the shell-to-base connection which have not been tested experimentally.

## ACKNOWLEDGEMENTS

The authors would like to acknowledge the financial support provided by CARBURA and the Swiss Federal Office for the Environment (OFEV).

## REFERENCES

- Clough, D.P., Clough, R.W. (1978). Earthquake Simulator Studies of Cylindrical Tanks. *Nuclear Engineering and Design* 46. California, USA.
- Coffin, Jr., L. F. (1954). A study of the effects of cyclic thermal stresses in ductile metals. *Trans. ASME* 76, 931–950.
- Cortes, G., and Nussbaumer, A. (2010). Seismic behavior of shell-to-base connections in large storage tanks. Rapport de mandat No. IC 495-1. Submitted to Carbura and Swiss Federal Office for the Environment (OFEV).
- Cortes, G., Nussbaumer, A., Berger, C., and Lattion, E. (2011). Experimental determination of the rotational capacity of wall-to-base connections in storage tanks. *J. Constructional Steel Research*. **67**, 1174-1184.
- Eurocode-8 (1998). Part 4: Silos, Tanks, and Pipelines. ENV 1998-4, European Committee for Standardization, Brussels, Belgium.
- Fujikazu, S., Akira, I., Hajime, H., and Yukio, M. (1988). Experimental study on uplifting behavior of flat-based liquid storage tanks without anchors. *Proc. 9th World Conference on Earthquake Engineering*. Tokyo-Kyoto, Japan: 649-654.
- Krawinkler, H., Zohrei, M., Lashkari-Irvani, B., Cofie, N., Hadidi-Tamjed, H. (1983). Recommendations for Experimental Studies on the Seismic Behavior of Steel Components and Materials. Report No. 61.
- Malhotra, P.K. (2002). Cyclic-Demand Spectrum. *Earthquake Engineering and Structural Dynamics*. **31**, 1441-1457.
- Malhotra, P.K., Veletsos, A. S. (1994a). Beam Model for Base-Uplifting Analysis of Cylindrical Tanks. *J. of Structural Engineering*. **120:12**, 3471-3488.
- Malhotra, P.K., Veletsos, A. S. (1994b). Uplifting Analysis of Base Plates in Cylindrical Tanks. *J. of Structural Engineering*. **120:12**, 3489-3505.
- Malhotra, P.K., Veletsos, A. S. (1994c). Uplifting response of unanchored liquid-storage tanks. *J. of Structural Engineering*. **120:12**, 3524-3546.
- Manson, S. S. (1954). Behavior of materials under conditions of thermal stress, Technical Note 2933, National Advisory Committee for Aeronautics, Tennessee, USA.
- Mazzoni, S., McKenna, F., Scott, M.H., and Fenves, G.L. (2006). The Open System for Earthquake Engineering Simulation (OpenSEES) User Command-Language Manual. PEER. Univ. Calif., Berkeley, CA, ([HTTP://OPENSEES.BERKELEY.EDU](http://OPENSEES.BERKELEY.EDU)).
- Miner, M. A. (1945). Cumulative damage in fatigue. *Trans. ASME* 67, A159–A164.
- NZSEE (2009). Seismic Design of Storage Tanks. New Zealand National Society for Earthquake Engineering Wellington, New Zealand.
- Prinz, G.S., Nussbaumer, A. (2012). Seismic performance of unanchored liquid storage tank shell-to-base connections – Phase 2. Rapport de mandat No. 174640: Ecole Polytechnique Federale de Lausanne (EPFL), Lausanne, Switzerland.
- Sabetta, F., and Pugliese, A. (1996). Estimation of response spectra and simulation of nonstationary earthquake ground motions. *Bulletin of the Seismological Society of America*. **86:2**, 337-352.